A reaction norm for flowering time plasticity reveals physiological footprints of maize adaptation

Justine Drouault[1], Carine Palaffre[2], Emilie J. Millet[1], Jonas Rodriguez[1], Pierre Martre[1], Kristian Johnson[1], Boris Parent[1], Claude Welcker[1], Randall J. Wisser[1,3*]

[1]LEPSE, University of Montpellier, INRAE, Institut Agro Montpellier, Montpellier, FR

[2]Experimental Unit of Maize, INRAE, 40390 Saint Martin De Hinx, FR

[3]Department of Plant and Soil Sciences, University of Delaware, Newark, Delaware, USA

***Correspondence:** Randall J. Wisser, randall.wisser@inrae.fr

ORCIDs: EJM: 0000-0002-2913-4892; JR: 0000-0001-8693-1022; PM: 0000-0002-7419-6558; CW: 0000-0002-8275-1259; RJW: 0000-0003-1075-0115

Current address:

Emilie J. Millet: INRAE, UR1052 GAFL, 84143 Montfavet, France

Jonas Rodriguez: Syngenta Seeds, P.O Box 18300, Greensboro, North Carolina, USASyngenta Seeds, P.O Box 18300, Greensboro, North Carolina, USA

keywords: Adaptation, GxE, Envirotyping, Flowering time, Maize

Running title: Modeling plasticity in maize flowering

Date of submission: November 22, 2024

Number of tables and figures

Tables: 2
Figures: 4

Supplementary data

Tables: 1
Figures: 2
Files: 6

Abstract

Understanding how plant phenotypes are shaped by their environments is crucial for addressing questions about crop adaptation to new environments. This study focused on analyzing the genetic variability underlying genotype-by-environment interactions and adaptation for flowering time in maize. We developed the use of a physiological reaction norm for flowering time plasticity (PRN-FTP) modeled from multi-environment trial networks, with genotype-specific parameters putatively linked to different regulatory modules for flowering time. We show how genotype-specific differences in developmental responses to temperature fluctuations condition differences in photoperiod perceived among genotypes. This occurs not only across but also within common environments, as the perception of photoperiod is altered by variation in rates of development and durations for becoming sensitized to photoperiod. Using a new metric for envirotyping sensed photoperiods for maize, it was found that, at high latitudes, different genotypes in the same environment can experience up to hours-long differences in photoperiod. This emphasizes the importance of considering genotype-specific differences in the experienced environment when investigating plasticity. Modeling the PRN-FTP for global breeding material of maize showed that tropical and temperate germplasm occupy distinct territories of the trait space for PRN-FTP parameters, supporting that the geographical spread and adaptation of maize was differentially mediated by distinct pathways for flowering time regulation. Our results have implications for understanding crop adaptation and for future crop improvement efforts.

Article Summary

Maize adjusts its flowering time across environments using genetic pathways tuned to cues like temperature and day length. This study models how different varieties perceive and respond to these factors, revealing that genotypes can perceive the same environment in distinct ways. By examining the physiological underpinnings of genetic and environmental interactions, the research highlights how maize's historical spread and artificial selection have shaped diverse strategies for flowering time regulation in tropical and temperate varieties.

Introduction

Plants exhibit vast phenotypic diversity, the principal axis for adaptation and evolution. The classic formalism $P = G + E + G \times E$ describes how phenotypes are determined by combinations of genetic (G) and environmental (E) effects. Environmental effects result from varying external conditions that lead to distinct phenotypic outcomes for the *same* genotype, a phenomena known as plasticity (Bradshaw, 1965). As 21st-century climate markedly shifts the environmental dimension to new frontiers, it is an important and opportune time to investigate plasticity (E) and genetic variation in plastic responses ($G \times E$). For crop improvement, harnessing plastic responses to shifts in climate conditions can facilitate the adaptation of crops into new territories or to alternative cropping systems (Rising and Devineni, 2020; Sloat *et al.*, 2020; Zabel *et al.*, 2021). Thus, approaches for modeling $G \times E$ that are rooted in the understanding of plasticity represent a promising direction for agricultural research (e.g., Millet *et al.*, 2019; Cooper *et al.*, 2020; van Voorn *et al.*, 2023).

The functional relationship that defines a pattern of plasticity across an environmental gradient is known as a reaction norm, with parameters that quantify the direction and magnitude of phenotypic change (Roof, 1997). The reaction norm provides a foundation for modeling phenotypic responses to the environment. However, separate disciplines have contemplated and conceived of reaction norms in different ways. A common approach in quantitative genetics uses the *Finlay–Wilkinson* statistical model (Finlay and Wilkinson, 1963), in which the phenotypic values of individual genotypes are regressed on an index defined by the mean values of all genotypes per environment. In this framework, typically, phenotypes are for final characteristics measured at the whole-plant scale that are targets for selection, such as flowering time, plant height, or yield. This method has provided a convenient generalization for modeling reaction norms from multi-environment trials (METs) where large collections of genotypes can be simultaneously tested across different field environments, enabling a widescale analysis of $G \times E$ (Jarquín *et al.*, 2014; Kusmec *et al.*, 2017; Guo *et al.*, 2023). Clearly, however, the environment is abstractly defined and confounded with latent environmental effects where mechanisms underlying $G \times E$ become elusive, resulting in a lack of biological interpretability. In contrast, focused on phenotyping of finer-scale traits in controlled settings, ecophysiologists have characterized norms of reaction for physiological responses to specific environment variables, such as the non-linear response of growth and development to temperature (Parent *et al.*, 2010; Parent and Tardieu, 2012). Embedding formalisms for these reaction norms in crop growth models allows an upscaling to final characteristics, modeled as an emergent outcome built upon biological mechanisms that dynamically drive plant development in response to environmental conditions (Muller and Martre, 2019). This method provides biological perspective, but studying broad diversity ($G \times E$) is challenged by experimental constraints to measuring the parameters of physiological reaction norms. In our study, we hypothesized that parameterizing a physiological reaction norm from MET data would allow us to analyze the diversity of flowering time plasticity in maize (*Zea mays* subsp. *mays*) and provide unique insights into maize adaptation.

The control of flowering time is regulated by a modular molecular network controlling physiological responses in development to multiple external signals, particularly temperature and photoperiod (Simpson and Dean, 2002; Colasanti and Coneva, 2009; Blümel *et al.*, 2015; Lee *et al.*, 2021). The influence of temperature results in a speeding or slowing of development, while, for photoperiod sensitive genotypes, the influence of photoperiod results in the suppression of reproductive transition and a delay in flowering time. Responses to temperature occur throughout a plant's life cycle, while the response to photoperiod is growth-stage specific. In maize, a facultative short-day (SD) species, the stage at which plants become sensitized to photoperiod is not directly observable, but based on photoperiod-swap experiments has been found to occur just prior to the timing of tassel initiation

(reproductive transition) when plants are grown in SD conditions (Kiniry *et al.*, 1983*a*,*b*). Above a critical photoperiod, under long-day (LD) conditions, tassel initiation in photoperiod sensitive genotypes is delayed beyond the timing at which they reach their sensitized stage. Thus, as physiological responses to temperature fluctuations across the development cycle interact with genotypic variation in rates of plant development and durations of the reproductive transition, different genotypes can reach the sensitized stage on different days, and therefore perceive different photoperiods, even within the same environment. For photoperiod sensitive genotypes, genotypic variation in photoperiod sensitivity creates additional plasticity, culminating in the formation of $G \times E$ interactions in flowering time across environments.

The current study was centered on the modeling and analysis of a physiological reaction norm for flowering time plasticity (PRN-FTP) that integrates the combined effects of genotype-specific responses to temperature and sensing of photoperiod underlying flowering time $G \times E$. Extending previous work (Kiniry *et al.*, 1983*a,b*; Choquette *et al.*, 2023), this was formulated as a bilinear, threshold-dependent function for the relationship between thermal time from crop emergence to male flowering (anthesis; $T_{\mathrm{t}}^{\mathrm{em-ant}}$) and a new environmental index for sensed photoperiod (DL^{s}). The DL^{s} index was developed to define the genotype-specific stage of photoperiod sensitivity and used to examine variation in photoperiod perceived by diverse genotypes of maize within and across environments of the Northern Hemisphere. We demonstrate how the PRN-FTP allows the decoupling of different components of flowering time regulation: (i) flowering time *per se*; (ii) critical photoperiod; and (iii) photoperiod sensitivity; with genotype-specific parameters estimated from MET data.

Finally, parameters of the PRN-FTP may be used to understand how components of flowering time plasticity mediate adaptation to novel environments, and how this in turn changes genotype plasticity for the future. Historical varieties of maize that spread 2000-5000 years ago from their tropical origins into temperate zones required flowering time adaptations to cooler climates with longer photoperiods (Tenaillon and Charcosset, 2011). Here, we show that the trait space relating variation in flowering time *per se* and photoperiod sensitivity for separate breeding pools reveals how selection history has shaped the plasticity of modern maize.

Materials and Methods

Experimental datasets

Summarized in Table S1, datasets ("D") from multiple projects and experiments were assembled to: (D1) select a temperature response function for thermal time estimation; (D2) estimate variation in the thermal time duration between crop emergence and tassel initiation ($T_{\mathrm{t}}^{\mathrm{em-TI}}$) in order to develop an index for sensed photoperiod (DL^{s}); (D3) envirotype DL^{s} in maize fields across the Northern Hemisphere; (D4) demonstrate methods for modeling a physiological reaction norm for flowering time plasticity (PRN-FTP); and (D5) compare the trait space of parameters estimated from the PRN-FTP in a diversity panel constituting separate breeding pools of maize. The current study focuses on days to anthesis (male flowering) as the final characteristic.

(D1) Three temperature response functions (Methods S1, Eq. S1-S3) for measuring thermal time were compared using MET data with 24 hybrids tested in 25 to 26 field environments, spanning latitudes from 30.5371°N to 44.2089°N (File S1; data sourced from the Genomes-To-Fields Initiative). For each environment, the sowing date, field coordinates, and best linear unbiased estimates (BLUEs) for calendar days from sowing to anthesis were obtained from McFarland *et al*., 2020 and Rogers *et al*.,

2021. Using temperature data, genotype-specific BLUEs for calendar days to anthesis were converted to thermal time.

(D2) A collection of 284 maize inbred lines (panel 1) was used to estimate $T_{\mathrm{t}}^{\mathrm{em-TI}}$ for each genotype using a physiological formalism (Eq. 1) based on experimental data for crop emergence, phyllochron, and final leaf number recorded in two experiments with short-day (SD) conditions that (File S2). Crop emergence and phyllochron were measured in a greenhouse phenotyping platform at the LEPSE of INRAE (PhenoArch, Montpellier, FR; Cabrera-Bosquet *et al.*, 2016) under well-watered conditions, while final leaf number was recorded in a field experiment in Puerto Vallarta, MX, also in well-watered conditions. For both experiments, daylengths throughout the growth cycle never exceeded 12.5 h. Additional details for these experiments can be found in Supplemental Information (Methods S2).

(D3) Computational envirotyping of DL^{s} was performed for fields across the Northern Hemisphere (latitudinal range of 13.7578 °N to 54.2900 °N) where maize was previously grown. For this, the geographical coordinates and planting dates of 671 field environments were assembled from past publications and ongoing projects (File S3).

(D4) To test modeling procedures for the PRN-FTP, anthesis data from 37 field trials were combined into a multi-environment trial (MET) dataset (File S4). This dataset maximized the number of field trials available for a common subset of genotypes also present in dataset D2 (so that genotype-specific values for DL^{s} could be determined), including seven temperate inbred lines (B37, B73, M37W, Mo17, Oh43, LH123Ht, and 2369) and seven tropical inbred lines (CML10, CML258, CML277, CML341, CML373, Tzi8, and Tzi9). Still, representation of these lines across the 37 environments was not fully balanced. The temperate lines were present in a minimum of 15 and a maximum of 22 environments. The tropical lines were present in a minimum of 18 and a maximum of 37 environments.

(D5) To examine the relationship between PRN-FTP parameters associated with flowering time *per se* and photoperiod sensitivity, MET data for a collection of 111 temperate, 52 tropical, and 51 admixed inbred lines constituting separate breeding pools (panel 2; Flint-Garcia *et al*., 2005) was assembled from previous experiments (File S5). These lines were observed across a maximum of three SD environments (maximum photoperiod <12.3 h) and 16 long-day (LD) environments (minimum photoperiod of >14.5 h) spanning 18.00 °N to 42.76 °N latitude.

Environmental data

For field trials considered in this study, temperature data were acquired from ground and satellite data sources for a common reference point of 2 m height. Ground data were obtained mostly from weather stations at a given field location. In two cases, ground data from a nearby airport within 5 km of the experimental field site was obtained from Weather Underground (https://www.wunderground.com/). Satellite data (weather variable 'T2M'; spatial resolution of ½° latitude x ⅝° longitude) was acquired from the R package *nasapower* (Sparks, 2018) using the latitude and longitude coordinates for each field location.

The photoperiod based on civil twilight at a given location for a given day of the year was acquired from the R package *TrenchR* (Buckley *et al.*, 2023). This uses the CBM daylength model described by Forsythe *et al.* (1995).

Comparison of temperature response functions

Three temperature response functions were compared for calculating thermal time (Eq. S1-S3). Comparisons were made based on the normalized root mean square error (NRMSE, normalized by the difference between maximum and minimum values) for the overall mean thermal time from sowing to anthesis. The NRMSE was estimated for each of the 24 hybrids in dataset D1 in order to identify the response function that minimized the mean NRMSE among all hybrids. The analyzed set of hybrids were from crosses between temperate-adapted lines classified as photoperiod insensitive, such that variation in anthesis dates (calendar days) across environments were expected to be primarily due to differences in temperature. Therefore, the magnitude of residual variation per hybrid was expected to reflect deviations from the model for temperature response. For the purpose of comparing different models for thermal time estimation with the same dataset, we assumed the influence of any latent variables on growth and development could be ignored.

Physiological reaction norm for flowering time

The PRN-FTP defined here was reformulated from a previous model by Kiniry *et al.* (1983*a*) that described the relationship between photoperiod conditions (x-axis) and thermal time from crop emergence to tassel initiation based on temporal dissections of shoot apical meristems ($T_{\mathrm{t}}^{\mathrm{em-TI}}$; y-axis). Kiniry *et al.* (1983*a*) used growth chambers in which constant levels of photoperiod were applied throughout the plant's growth cycle. However, in the setting of MET networks considered here, photoperiods are not constant (DL^{s} depends on the day of year a plant become sensitized to photoperiod in a given environment) and estimating tassel initiation from dissections of meristems is not practical at large scale (rather, in METs, days to flowering are routinely recorded). Since there is no known visible marker for when plants become sensitized to photoperiod, we devised DL^{s} as a proxy measure based on previous findings showing that the stage of initial sensitization closely corresponds to the BVP-ti (i.e., the $T_{\mathrm{t}}^{\mathrm{em-TI}}$ measured under SD conditions; Kiniry *et al.*, 1983*b*). Thus, we define the PRN-FTP as the relationship between the proxy measure for DL^{s} (x-axis) and thermal time from crop emergence to anthesis ($T_{\mathrm{t}}^{\mathrm{em-ant}}$; y-axis).

The PRN-FTP was modeled for MET datasets D4 and D5. For trial environments with data on crop emergence, the specific date of emergence was used. For trials without this information, dates of emergence were predicted based on a cumulative thermal time from sowing to emergence of 76 °Cd (estimated using Eq. S2 using emergence data from 15 environments sourced from the Maize ATLAS project [Choquette *et al.*, 2023]).

Estimation of sensed photoperiod. We used an empirical approach to estimate genotype-specific values for DL^{s} across environments, which were independent of the $T_{\mathrm{t}}^{\mathrm{em-ant}}$ values obtained from MET data. DL^{s} was determined by first calculating $T_{\mathrm{t}}^{\mathrm{em-TI}}$ (Eq. 1) for a panel of 284 genotypes grown in SD conditions (Methods S2; dataset D2). The panel included a diverse set of tropical, semi-tropical, and temperate lines, many of which exhibit photoperiod sensitivity. By growing these plants under SD conditions, the delayed-development response to photoperiod in sensitive genotypes is not activated. Following Kiniry *et al.* (1983*a*), the SD-$T_{\mathrm{t}}^{\mathrm{em-TI}}$ is considered the basic vegetative phase required to reach tassel initiation (BVP-ti), which we used to develop the DL^{s} index.

Considering that tassel initiation occurs on the day when the last leaf primordium is formed (Lejeune and Bernier, 1996) and that rates of leaf primordia formation and leaf tip appearance are proportional (Padilla and Otegui, 2005), $T_{\mathrm{t}}^{\mathrm{em-TI}}$ can be calculated as:

$$T_{\mathrm{t}_i}^{\mathrm{em-TI}} = \frac{P_{\mathrm{tip}_i}}{\alpha_{\mathrm{phyll/plast}}}\left(L_{\mathrm{F}_i} - L_{\mathrm{pri}}^{\mathrm{em}}\right) \qquad \text{(Eq. 1)}$$

where, $T_{\mathrm{t}_i}^{\mathrm{em-TI}}$ (°Cd) is the cumulative thermal time from crop emergence to tassel initiation of the ith genotype, P_{tip_i} (leaf °Cd^{-1}) is the phyllochron of the ith genotype (i.e., the thermal time between the appearance of two successive leaf tips), L_{F_i} (leaf) is the final leaf number of the ith genotype, $\alpha_{\mathrm{plast/phyll}}$ (dimensionless) is a constant ratio of phyllochron to plastochron (i.e., the thermal time between the formation of two successive leaf primordia), and $L_{\mathrm{pri}}^{\mathrm{em}}$ (primordium) is a constant number of primordia formed at crop emergence. Genotype-specific values for P_{tip_i} and L_{F_i} were obtained from dataset D2 on panel 1 (Methods S2). For maize, $\alpha_{\mathrm{plast/phyll}}$ may range from 1.58 to 1.85 (Kiniry, 1991; Lejeune and Bernier, 1996; Padilla and Otegui, 2005; Andrieu *et al.*, 2006). In this study, we set it at the average value reported in the literature (1.73). There are four to five leaf primordia in the embryo of maize seeds (Bonnett, 1954; Padilla and Otegui, 2005), and between germination and crop emergence about two other leaf primordia are formed (Padilla and Otegui, 2005). Thus, here, $L_{\mathrm{pri}}^{\mathrm{em}}$ was set equal to 5.5 primordia.

Finally, given the emergence date (measured or predicted), the genotype specific $T_{\mathrm{t}}^{\mathrm{em-TI}}$ and the temperature records for each specific environment were used to predict the calendar day that a given genotype becomes sensitized to photoperiod. In turn, the photoperiod of the specific calendar day in that environment was predicted using the R package *TrenchR* (Buckley *et al.*, 2023) to obtain the DL^{s}.

Estimation of thermal time from crop emergence to tassel initiation. Estimates for $T_{\mathrm{t}}^{\mathrm{em-ant}}$ were computed as cumulative thermal times from dates of emergence (observed or predicted) to dates of anthesis determined from BLUEs of days to anthesis.

Envirotyping of sensed photoperiod

Dataset D3 was used to computationally envirotype DL^{s} for maize across cultivation areas in the Northern Hemisphere. Across and within environments, DL^{s} was quantified for three maturity groups, defined by the lower (5th), median (50th), and upper (95th) percentiles of the $T_{\mathrm{t}}^{\mathrm{em-TI}}$ distribution estimated for panel 1 (Table 1). For each percentile-maturity group, the specific value of $T_{\mathrm{t}}^{\mathrm{em-TI}}$ was used to predict corresponding DL^{s} values per environment. To examine how temporal changes in photoperiod within an environment influences the DL^{s} of different genotypes, in each environment, differences in DL^{s} between the separate maturity groups was compared to the environment-specific rate of photoperiodic change. The rate was computed from photoperiod values on the single days flanking the day of DL^{s} for the 50th percentile-maturity group.

In a typical application, the PRN-FTP would be constructed for each of the genotypes tested in the MET. While $T_{\mathrm{t}}^{\mathrm{em-ant}}$ are specific to the observations on each genotype, DL^{s} could be defined for each specific genotype or a common reference genotype. The choice depends on whether different genotypes in the same environment experience large or small differences in photoperiod. Therefore, a sensitivity analysis was performed to assess the impact of using genotype-specific values versus a common reference value for DL^{s}.

Statistical analysis of the PRN-FTP

Bilinear statistic for estimating parameters of the PRN-FTP. With a sufficient coverage of DL^{s} spanning SD and LD environments, we modeled the PRN-FTP using a continuous two-phase (bilinear) regression model with threshold detection (Fong *et al.*, 2017*a*). Here, using the R package *chngpt* (Fong *et al.*, 2017*b*), the "hinge model" was fit to the PRN-FTP for each genotype in dataset D4.

$$T_{\mathrm{t}}^{\mathrm{em-ant}} = \alpha + \beta(DL^{s} - e)_{+} \quad \text{(Eq. 2)}$$

where $T_{\mathrm{t}}^{\mathrm{em-ant}}$ is the response variable; e is the threshold parameter; DL^{s} is the sensed daylength with a threshold effect; $I(DL^{s} > e) = 1$ when $DL^{s} > e$ and 0 if $DL^{s} \leq e$; $(DL^{s} - e)_{+}$ denotes the hinge function, which equals $DL^{s} - e$ for $DL^{s} > e$ and 0 otherwise; and α and β are the intercept and slope parameters, respectively. The model was fitted using default settings, with no constraints set for estimating the threshold value (breaking point of the bilinear model). Estimated effects include an intercept, threshold value, and slope, which correspond to physiological components of flowering time: the flowering time *per se*, the critical threshold for photoperiod sensitivity, and the degree of photoperiod sensitivity, respectively.

Correction for latent variables affecting thermal times to anthesis. If only temperature influenced the flowering time of a photoperiod insensitive genotype, their $T_{\mathrm{t}}^{\mathrm{em-ant}}$ would be nearly the same across an MET. In our experience, this simplistic assumption often does not hold in MET data (as confirmed with dataset D1), but aside from measurement error the cause for deviations can be due to various possibilities, including the influence of other environmental factors, differences in crop management practices, differences between air temperature and the temperature sensed by the crop, imprecision and biases in weather data, or other latent variables. Therefore, with dataset D4, we tested an alternative approach using photoperiod insensitive control lines to adjust for across environment latent variable effects prior to constructing the PRN-FTP.

Seven photoperiod insensitive temperate genotypes were defined as control lines. The 37 environments for dataset D4 were assembled from different experiments but unfortunately did not include all seven control lines in all environments, so two sets of control groups were defined (set 1: B37, B73, M37W, Mo17, and Oh43; set 2: LH123Ht and 2369). Sets 1 and 2 were associated with 22 and 15 of the environments, respectively. For each set, the overall mean of $T_{\mathrm{t}}^{\mathrm{em-ant}}$ was calculated across environments of the MET in which they were associated. The environment-specific residuals were then used to adjust the thermal times for the remaining non-control genotypes in each of the corresponding environments of the MET. We note that using two sets of control lines that were also imbalanced across environments (see above) could introduce some bias and is not ideal, but our aim was to test this approach.

Analysis of flowering time plasticity in a diversity panel

We sought to investigate the trait space relationship between the PRN-FTP parameters flowering time *per se* and photoperiod sensitivity in a collection of maize lines adapted to different geographical zones (panel 2; dataset D5). However, the MET lacked sufficient coverage of DL^{s} to estimate critical threshold values for the PRN-FTP using the hinge model. Therefore, an "LD-SD" method of simple linear regression was used in which latent-variable adjusted BLUEs for $T_{\mathrm{t}}^{\mathrm{em-ant}}$ (response variable) were regressed on contrasting means of DL^{s} for the two sets of SD (range of 11.9 h to 12.4 h) and LD (range of 14.5 to 16.5 h) environments (predictor variable). Latent variable adjustment was applied as described above, using the same D4 control lines from set 1, and DL^{s} values were computed based on the 50th-percentile reference for $T_{\mathrm{t}}^{\mathrm{em-ant}}$ in panel 1 (we did not have data to estimate genotype-specific values for $T_{\mathrm{t}}^{\mathrm{em-ant}}$ in panel 2). The LD-SD model assumes a common photoperiod threshold corresponding to the mean of DL^{s} among all SD environments exists for all genotypes. In dataset D5, not all genotypes were observed in all environments, such that DL^{s} means used for regression analysis varied slightly by genotype according to the sets of environments for which data were available. When fitting the LD-SD linear regression model, the DL^{s} means were offset to zero so that the intercept was estimated at the mean SD-DL^{s} value for the corresponding genotype. For the LD-SD method, we define

genotype-specific estimates of the intercept and slope as corresponding parameters for flowering time *per se* and photoperiod sensitivity.

Results

Choosing a temperature response function to construct the PRN-FTP

Thermal time is used to determine DL^s and T_t^{em-ant} to formulate the PRN-FTP function, such that different temperature response functions for calculating thermal time could result in different outcomes. A comparison of three different temperature response functions showed no significant difference in the NRMSEs for thermal times to anthesis for 24 photoperiod-insensitive hybrids tested in 25 to 26 environments in North America. Regardless of the temperature response function that was tested, for each hybrid, the environment-specific thermal time to anthesis deviated, on average, by ~10% (range 9 to 13%) from the across-environment mean (Fig. S1). Therefore, for the current study, we chose the non-linear response function by (Wang and Engel, 1998) adapted for maize (Eq. S2) due to its common implementation in crop growth models (Wang *et al.*, 2017), its higher physiological realism compared with the linear response function (Eq. S1), and its greater flexibility compared to the Arhenus model (Parent *et al.*, 2010).

Predicting when maize becomes sensitized to photoperiod

There is no known visible marker to measure the timing when maize plants become sensitized to photoperiod for determining DL^s. Thus, we defined this timing as T_t^{em-TI} measured under SD conditions since this closely corresponds to the photoperiod sensitized phase (Kiniry *et al.*, 1983*b*). An issue is that directly observing tassel initiation requires temporal dissections of shoot apical meristems which is not possible at a large scale. To circumvent this, we used an ecophysiological formalism to predict genotype-specific values for T_t^{em-TI} (Eq. 1) of the 284 genotypes in panel 1 grown under SD conditions (dataset D2; File S2). Under the same growth conditions, for eight genotypes from the same panel, this was validated in a separate experiment to interpedently quantify T_t^{em-TI} from microscopy data on differentiation of shoot apical meristems into tassel primordia (Methods S2). The Pearson correlation coefficient between predicted and observed BVP-ti values was 0.84, indicating the formalism-based predictions for T_t^{em-TI} align closely with observational data. Table 1 summarizes percentiles of the distribution for predicted values of T_t^{em-TI} in panel 1, with the 5th, 50th, and 95th percentile values used to represent early, medium, and late maturity groups for envirotyping DL^s.

Spatiotemporal variation in the sensed photoperiod for maize

DL^s integrates information on sowing dates, emergence dates, developmental responses to temperature, the temperature and photoperiodic conditions of an environment, and the genetic diversity for the physiological traits underlying flowering time. This can be used to understand how different genotypes sense photoperiod across and within environments, and how this varies according to spatiotemporal patterns in climate and weather. To examine how photoperiods are perceived by maize, we computationally envirotyped DL^s for 671 field environments across the Northern Hemisphere where maize has been previously grown (Fig. 1).

We first summarized the spatial axis of variation in DL^s using the 50th percentile of T_t^{em-TI} (326 °Cd) in panel 1 as a common reference for envirotyping (Table 1; Fig. S2). The maximum difference in DL^s among all environments was 6.4 hours with a range from 11.9 to 18.3 h (Fig. 1a). For regions above 30° N, corresponding to the majority of MET locations used for maize research and production in the

USA and Europe (Figure 1a-b), we examined how DL^s for maize differs between continents. Mean DL^s across the USA was 16.12 h and in Europe was 16.68 h, with lower (5-percentile) to upper (95-percentile) ranges of 14.35 to 16.37 and 15.73 to 17.46, respectively. These spatial patterns are primarily driven by climatic variation in photoperiod across latitude coupled with the seasonality for maize cultivation. Interannual differences in temperature and planting dates at the same location can give rise to additional variation in DL^s for maize. To examine this, we selected 118 field sites where maize was planted for at least two years and found that DL^s within a single location varied by as much as 1.7 hours, with a mean absolute difference of 0.27 h.

Next, we questioned the extent to which multiple genotypes grown within the same field environment perceive a different photoperiod. Beyond the equator, photoperiod is not constant across days of the year, with increasing rates of daily change in association with latitude. Therefore, genotypes differing in $T_{\mathrm{t}}^{\mathrm{em-TI}}$ that reach their photoperiod sensitized stage on different days would perceive a different photoperiod (Fig. 1b-c), but to our knowledge the magnitude by which this varies has not been investigated. Using the 5th (239 °Cd) and 95th (434 °Cd) percentiles of $T_{\mathrm{t}}^{\mathrm{em-TI}}$ in panel 1 to represent early and late percentile-maturity groups, the DL^s at these limits frequently differed by more than 1 h, with the largest difference reaching 3.78 h (Fig. 1b). Differences in DL^s above 2 h were rare and occurred only in locations at high latitudes where late genotypes are not cultivated for maize production. Nevertheless, this highlights how the genetic diversity of maize can intersect with environmental variation within the same field, leading to differences in the photoperiod to which genotypes respond.

If the 50th-percentile for $T_{\mathrm{t}}^{\mathrm{em-TI}}$ is used as a common reference for envirotyping DL^s, the magnitude of inaccuracy in genotype-specific DL^s varies according to the set genotypes per environment. For instance, the early and late percentile-maturity groups differed from the 50th percentile reference by as little as no difference to as much as 1.41 h and 2.40 h, respectively (File S3). The larger differences occurred at higher latitudes where rates of photoperiodic change were greatest. This reduced to zero as a function of the rate of photoperiodic change (Fig. 1d).

Using METs for modeling the PRN-FTP

To test approaches for modeling the PRN-FTP from METs, we combined flowering time data from multiple projects totaling 37 field experiments (dataset D4) that included, albeit with imbalanced data (Table S1), a common set of seven genotypes of tropical origin that were expected to be photoperiod sensitive. This was used to compare procedures for estimating genotype-specific PRN-FTP parameters for flowering time *per se* (intercept), critical photoperiod (threshold), and photoperiod sensitivity (slope) using a two-phase regression model (see Methods; Fig. 2).

Using MET data to construct the PRN-FTP makes the simplistic assumption that physiological sensitivities to temperature and photoperiod are the only environmental factors influencing flowering time. Although these are dominant factors, other variables can also affect maize growth and development, but the specific causes are often unknown and likely to vary from one field environment to another. Therefore, we devised an approach to control for latent effects on flowering time and evaluated how adjusted values for the $T_{\mathrm{t}}^{\mathrm{em-ant}}$-phenotypic axis affected PRN-FTP parameter estimation. Using a designated set of photoperiod-insensitive control genotypes present in the D4 MET, their overall mean $T_{\mathrm{t}}^{\mathrm{em-ant}}$ across environments was defined as an expected value for the specific effect of temperature on flowering time (i.e., for photoperiod insensitive genotypes, $T_{\mathrm{t}}^{\mathrm{em-ant}}$ is expected to be the same across environments, with deviations attributed to latent variables; see Materials and Methods). Then, environment-specific deviations from the overall mean were used to

adjust the $T_{\mathrm{t}}^{\mathrm{em-ant}}$ values for the remaining lines in each of the corresponding environments. Fig. 2 portrays this procedure and how it affects estimates for the PRN-FTP parameters.

When tested using genotype-specific DL^{s} values for each of the seven tropical genotypes, latent variable adjustment of $T_{\mathrm{t}}^{\mathrm{em-ant}}$ enhanced the precision of the overall model fit of the PRN-FTP by an average of two-fold (Table 2). Using adjusted values also led to changes in the estimated thresholds of sensitivity, which in turn resulted in differences in the estimated flowering times *per se* by as much as 5% and slopes of sensitivity by as much as 77% (Table 2).

As described in the previous section, different genotypes can experience different photoperiods within environments, such that points along the DL^{s}-environmental axis of the PRN-FTP may differ among genotypes in a common MET. This caused us to question the standard approach to modeling reaction norms from METs where all genotypes are assumed to experience the same environmental conditions in each field. If the specific conditions experienced by different genotypes are sufficiently large, this could impact parameter estimates of a reaction norm. To test this, we compared modeling the PRN-FTP using the latent-adjusted values for $T_{\mathrm{t}}^{\mathrm{em-ant}}$ with the DL^{s} predictor based on common values from the 50th percentile reference. The lines presented adequate variation for testing this: compared to the 50th-percentile reference point, the genotype-specific values of $T_{\mathrm{t}}^{\mathrm{em-TI}}$ used for estimating DL^{s} ranged from the 37th to 95th percentiles of the $T_{\mathrm{t}}^{\mathrm{em-TI}}$ distribution in panel 1. However, the set of environments in the MET network of dataset D4 presented smaller contrasts in DL^{s} than would occur at higher latitude (European) environments (Fig 1b): the largest difference in DL^{s} between these specific genotypes and the common reference was 0.22 h. In this case, changes in coefficient estimates for thresholds of sensitivity and flowering time *per se* were negligible, but the slope parameter for photoperiod sensitivity changed by 12% for one of the lines (Table 2). Nevertheless, these results show that intra-environment variation in DL^{s} among genotypes can affect PRN-FTP parameters estimated from MET data. Even for this small sample of genotypes, Fig. 3 highlights a wide range of diversity for flowering time plasticity in maize consisting of unique parameterizations of the PRN-FTP.

Relating components of the PRN-FTP to understand maize adaptation

Since flowering time *per se* and photoperiod sensitivity underlie flowering time adaptation across environments (Choquette *et al.*, 2023), we questioned how the trait space of these PRN-FTP parameters is structured among primary breeding pools of maize. For this, we assembled an MET dataset (D5) from 19 field trials with a common set of inbred lines consisting of tropical, temperate, and admixed breeding material. Computational envirotyping showed that DL^{s} for the D5 MET was restricted to two small intervals of photoperiod conditions, with three environments of 11.9 to 12.4 h photoperiod and 16 environments of 14.5 to16.5 h photoperiod. With a large gap in coverage of DL^{s}, the two-phase regression function for the PRN-FTP could not be reliably fit. In this case, the PRN-FTP was modeled using an LD-SD method based on simple linear regression after, as previously described, adjusting for latent variables with the same control lines described previously. Examining the relationship between flowering time *per se* and photoperiod sensitivity showed that temperate and tropical material occupy distinct territories of the trait space (Fig. 4; File S6). Temperate lines tend to have a lower flowering time *per se* and nearly no photoperiod sensitivity, while tropical lines tend to have a higher flowering time *per se* coupled with a large range in photoperiod sensitivity. Fitting genetic expectations for polygenic traits, genotypes with admixed ancestry are positioned between the two.

Discussion

Understanding trait plasticity is important for adapting crops to new environments. To study the variation in plastic responses, METs allow large collections of genotypes to be characterized across environmental gradients. However, as demonstrated in this study, due to phenological variation and stage-specific sensitivities, different genotypes within each field environment may not experience identical environmental conditions. This can complicate the definition of environmental indices for modeling reaction norms from METs, challenging standard approaches that assume a common environment is sensed by all genotypes. Based on the ecophysiology of maize flowering time, the current study defines a new metric, DL^s, for quantifying the specific photoperiods sensed by different genotypes within and across environments. Using DL^s to envirotype maize fields in the Northern Hemisphere, we showed that, at high latitudes, where cooler temperatures that slow development combine with relatively large daily rates of photoperiodic change, genotypes in the same environment can experience more than a 1 h difference in DL^s (Fig. 1). This occurs more often and is more pronounced across maize environments in Europe than in the U.S. due to higher rates of photoperiod change (Fig. 1d). Thus, to provide more accurate information about the variation in trait plasticity, the construction of genotype-specific reaction norms for flowering time and other traits should be considered on a case-by-case basis.

Constructing the PRN-FTP from METs is the most practical approach for studying the diversity of flowering time plasticity, but this is challenged by the geographical structure of photoperiod (Fig. 1) and the sensitivity of parameter estimation to gaps in DL^s (Table 2, Fig. 3). Characterizing the full scope of flowering time plasticity therefore requires testing across numerous field sites spanning nearly an entire hemisphere to capture a sufficient range and density of DL^s. However, we found that currently available MET datasets for maize do span LD and SD conditions but have limited to no coverage of DL^s from 12.4 to 14.5 h, the specific range for expected variation in the critical photoperiod for maize (Rood and Major, 1980; Kiniry *et al.*, 1983*a*). In this case, an alternative approach is to split METs into sets of LD and SD scenarios by assuming a common threshold across all genotypes (Coles *et al.*, 2010; Hung *et al.*, 2012), where parameters for flowering time *per se* and photoperiod sensitivity can be estimated by linear regression as the intercept and regression coefficient, respectively. Nonetheless, with scant information on critical photoperiods for maize, and given the dependence of accurate threshold estimation for regression analysis of the PRN-FTP (Table 2), envirotyping with DL^s could be used to design new METs for future research on flowering time plasticity.

The PRN-FTP provides a parsimonious model for flowering time plasticity, taking into account the dominant effects of temperature and photoperiod. However, in METs, latent variables can affect flowering time, requiring appropriate adjustments. In particular, constructing the PRN-FTP from thermal time estimates can be obscured by the influence of other factors besides temperature on growth and development, such as drought (e.g., Harrison *et al*., 2014; Herrero and Johnson 1981). To address this issue, we applied a between-environment covariate adjustment using photoperiod-insensitive control lines that were expected to have the same thermal time to anthesis across the full range of DL^s. This consistently resulted in a more precise fit of the bilinear response function for the PRN-FTP (Table 2; Fig. 2). Nevertheless, it is important to acknowledge that the choice of a control group could introduce some bias, as it may uniquely vary in other ecophysiological responses. Another challenge in modeling the PRN-FTP is that not all genotypes exhibit a clear bilinear response. For example, photoperiod-insensitive genotypes only display differences in flowering time *per se*, rendering the two-phase regression function invalid. In such cases, linear regression using the LD-SD method is the most appropriate way of capturing the relationship between $T_{\mathrm{t}}^{\mathrm{em-ant}}$ and DL^s. Thus, while the PRN-FTP model offers a valuable framework for understanding flowering time plasticity, careful consideration of latent variables, choice of control group, and genotype-specific responses is necessary for accurate

476 modeling. Incorporating additional factors and exploring alternative models may further improve the
477 utility of the PRN-FT model for applications in plant science.

478 A large body of work has elucidated a generally conserved molecular network for flowering time
479 regulation in plants, involving a set of semi-independent pathways that converge on the genetic control
480 of shoot apical meristem identity and anthesis date (Srikanth and Schmid, 2011; Dong *et al.*, 2012). In
481 several crops including maize, there has been significant progress in understanding the multigenic
482 architectures for variation in days to flowering time and photoperiod sensitivity (Buckler *et al.*, 2009;
483 Hung *et al.*, 2012; Yang *et al.*, 2013), reflective of the complex network structure of flowering time
484 regulation. We propose that constructing and decomposing the PRN-FTP from METs on large
485 collections of genotypes can be used to unravel the variation linked to some of these specific pathways.
486 Estimates for critical photoperiods and photoperiod sensitivities from the PRN-FTP can be expected
487 to capture interaction variation between the circadian clock and the photoperiod response pathways
488 (Itoh *et al.*, 2010), along with the possible partial effects of the gibberellic acid pathway suggested by
489 some observations (Johansson and Staiger, 2015; Izawa, 2021). Correcting for latent variables should
490 remove some of the effects of other environment-dependent responses that influence flowering time,
491 leading to more accurate estimates of the variation in the photoperiodic responses. We expect that
492 flowering time *per se* primarily reflects endogenous pathways including the autonomous, aging, and
493 gibberellic acid pathways, whereby flowering time is regulated independent of daylength (Minow *et*
494 *al.*, 2018). The use of thermal time, however, negates the analysis of variation arising from temperature
495 effects, which is an emerging pathway in the regulation of flowering time (Lee *et al.*, 2013; Jin *et al.*,
496 2023).

497 Predating the advent of modern varieties, populations of maize expanded from their tropical origins
498 into temperate zones (Tenaillon and Charcosset, 2011). This was facilitated by flowering time
499 adaptations, evidenced by selection on separate modules of the gene regulatory network for flowering
500 time (Gaudinier and Blackman, 2020). Distinct breeding pools for maize were then established from
501 locally preadapted populations, which have largely persisted as separate pools of tropical and temperate
502 maize. Thus, we reasoned that the PRN-FTP trait space of flowering time *per se* and photoperiod
503 sensitivity for modern varieties could be used to infer about historical selection on flowering time
504 pathways in maize. Figure 4 corroborates that distinct selection on these pathway-associated
505 components of flowering time has uniquely structured the plasticity in tropical and temperate maize.
506 However, the observed trend of reducing photoperiod sensitivity with flowering time *per se* is not
507 necessarily indicative of genetic or physiological coupling of the regulatory pathways, such that
508 genotypes with short flowering time *per se* and high photoperiod sensitivity could exist. Instead, this
509 appears to be a byproduct of the preadaptation history and subsequent breeding of maize. This is
510 supported by results from experimental evolution for early flowering time in tropical populations where
511 photoperiod sensitivity is rapidly eliminated while flowering time *per se* is continually shortened by
512 continued selection in LD environments of the temperate zone (Teixeira *et al.*, 2015; Choquette *et al.*,
513 2023). In contrast, selection in SD environments of the tropical zone apparently has no effect on
514 photoperiod sensitivity, where the longer growing seasons have limited the selection for a reduced
515 flowering time *per se*. This highlights how the PRN-FTP can be used for studying crop diversity, and
516 that knowledge about the historical context of adaptation and breeding is crucial for interpreting the
517 observed patterns in the PRN-FTP-derived trait space.

518 **Conclusions**

519 In this study, we explored various aspects of a physiological reaction norm for modeling flowering
520 time plasticity in maize. Envirotyping with DL^s is a valuable tool for examining the global distribution

of photoperiodic sensing in maize and constructing the PRN-FTP from MET data. Notably, the geographical distribution of current public MET networks for maize containing common sets of genotypes is concentrated in SD and LD environments with discontinuity in DL^{s} across the critical photoperiod range. This hinders investigation of the PRN-FTP parameter space for maize and accurate modeling of flowering time $G \times E$, warranting further experimentation. The DL^{s} index can be used for the design of new MET networks to address this.

The PRN-FTP model provides an ecophysiological framework for understanding variation in flowering time. For a specific genotype, the pace of development towards reproductive transition is affected by temperature fluctuations within an environment, with the magnitude of this influence varying across environments based on the unique temperature patterns. When contrasting genotypes are present in the same environments, interactions between temperatures and genetic variation in rates of development and durations of reproductive transition ($T_{\mathrm{t}}^{\mathrm{em-TI}}$) gives rise to variation in the timing of photoperiod sensitization. In turn, genetic variation in critical thresholds and photoperiod sensitivities lead to secondary interactions with daily rates of photoperiodic change within and across environments. In essence, as genotypes become sensitized to photoperiod at different times, genetic variation in their response to photoperiod further alters the timing of reproductive transition and flowering time, whether or not they are exposed to the same photoperiod within an environment. This highlights the intricate interplay between genetic and environment effects that shape the complex trait variation of flowering time.

Lastly, as the PRN-FTP model is based on common ecophysiological processes, we expect that it can be extended to other crops. Investigating the trait space of PRN-FTP components can provide valuable insights into flowering time adaptations in various species. Our findings underscore the significance of considering the historical context of adaptation and breeding in unraveling the genetic and physiological underpinnings of complex traits. This, in turn, holds promising implications for future crop improvement endeavors.

Acknowledgements: This study was made possible thanks to the production and availability of datasets from prior and ongoing projects: the EXPOSE and PhotoGrid projects at INRAE-LEPSE (ANR-16-IDEX-0006; France 2030 program; Post AgreenSkills Fund), the INVITE project (European Union's Horizon 2020 research and innovation program, grant no. 817970), the Maize ATLAS project (USDA-ARS, grant no. 2011-67003-30342), the Multiple Disease Resistance project (North Carolina State University, Cornell University, and University of Delaware collaboration), the Genomes-to-Fields Initiative (https://www.genomes2fields.org/home/), and the Panzea project (NSF-PGRP, grant no. 1238014). We wish to thank a number of people who contributed to this study: (i) Mainassara Abdou Zaman-Allah, Terence Molnar, and Prasanna Boddupalli from CIMMYT for providing much of the germplasm used for panel 1; (ii) Alexis Bédiée, Llorenç Cabrera-Bosquet, Nicole Choquette, Arnaud Desbiez-Piat, Thomas Laisné, Noé Lalouette-Marrier d'Unienville, Maëlle Lis, Anthony Rosello, Javier Soto Mendoza, and Benoît Suard for supporting the PhenoArch platform experiments at Montpellier, FR; (iii) Arnaud Brunet, Bernard Lagardere, and Jean-Rene Loustalot from the experimental station at Saint-Martin-de-Hinx, FR for supporting germplasm management and field testing; (iv) the ISRA team Ibrahima Sarr, Malick Ndiaye, Awa Mbengue, Abdoulaye Hoth, and Alain Audebert (CIRAD) for field trial data from Nioro du Rip, SN; and (v) the Moreno Retis team José Moreno and Luis Rodríguez for field trial data from Puerto Vallarta, MX.

Author Contributions: JD, RJW: conceptualization; CP, CW, RJW: resources; JD, CP, EM, RJW: investigation; JD, CP, JR, RJW: data curation; JD, PM, BP, RJW: methodology; JD, JR, KJ, RJW:

formal analysis; JD, RJW: writing - original draft; EM, JR, PM, KJ: writing - review & editing; BP, CW, RJW: supervision; EM, RJW: funding acquisition.

Conflict of Interest: The authors declare that the research was conducted in the absence of any commercial or financial relationships that could be construed as a potential conflict of interest.

Funding Statement: This work was supported by the French National Research Agency (ANR-16-IDEX-0006), the France 2030 program, project EXPOSE (PAF_18) supported by INRAE, and the European Union's Horizon 2020 research and innovation program, grant no. 817970.

Data Availability: Data and metadata from this study are available in Supplementary Files at Dryad (https://doi.org/10.5061/dryad.x95x69pth). Sources of external data are indicated in the methods sections. Code for fitting the PRN-FTP is available at: https://github.com/maizeatlas/prnftp.

References

Andrieu B, Hillier J, Birch C. 2006. Onset of sheath extension and duration of lamina extension are major determinants of the response of maize lamina length to plant density. Annals of Botany **98**, 1005–1016.

Blümel M, Dally N, Jung C. 2015. Flowering time regulation in crops-what did we learn from Arabidopsis? Current Opinion in Biotechnology **32**, 121–129.

Bonhomme R, Derieux M, Kiniry JR, Edmeades GO, Ozier-Lafontaine H. 1991. Maize Leaf Number Sensitivity in Relation to Photoperiod in Multilocation Field Trials. Agronomy Journal **83**, 153–157.

Bonnett OT. 1954. The inflorescences of maize. Science **120**, 77–87.

Bradshaw AD. 1965. Evolutionary significance of phenotypic plasticity in plants. phenotypic plasticity **23**, 207–215.

Buckler ES, Holland JB, Bradbury PJ, *et al.* 2009. The genetic architecture of maize flowering time. Science **325**, 714–718.

Buckley LB, Briones Ortiz BA, Caruso I, John A, Levy O, Meyer A V., Riddell EA, Sakairi Y, Simonis JL. 2023. TrenchR: An R package for modular and accessible microclimate and biophysical ecology. PLOS Climate **2**, e0000139.

Cabrera-Bosquet L, Fournier C, Brichet N, Welcker C, Suard B, Tardieu F. 2016. High-throughput estimation of incident light, light interception and radiation-use efficiency of thousands of plants in a phenotyping platform. The New phytologist **212**, 269–281.

Choquette NE, Holland JB, Weldekidan T, Drouault J, de Leon N, Flint-Garcia S, Lauter N, Murray SC, Xu W, Wisser RJ. 2023. Environment-specific selection alters flowering-time plasticity and results in pervasive pleiotropic responses in maize. New Phytologist **238**, 737–749.

Colasanti J, Coneva V. 2009. Mechanisms of floral induction in grasses: Something borrowed, something new. Plant Physiology **149**, 56–62.

Coles ND, McMullen MD, Balint-Kurti PJ, Pratt RC, Holland JB. 2010. Genetic control of photoperiod sensitivity in maize revealed by joint multiple population analysis. Genetics **184**, 799–812.

Cooper M, Tang T, Gho C, Hart T, Hammer G, Messina C. 2020. Integrating genetic gain and gap analysis to predict improvements in crop productivity. Crop Science **60**, 582–604.

Dong Z, Danilevskaya O, Abadie T, Messina C, Coles N, Cooper M. 2012. A gene regulatory network model for Floral transition of the shoot apex in maize and its dynamic modeling. PLoS ONE **7**.

Finlay KW, Wilkinson GN. 1963. The analysis of adaptation in a plant-breeding programme. Australian Journal of Agricultural Research **14**, 742–754.

Flint-Garcia SA, Thuillet AC, Yu J, Pressoir G, Romero SM, Mitchell SE, Doebley J, Kresovich S, Goodman MM, Buckler ES. 2005. Maize association population: A high-resolution platform for quantitative trait locus dissection. Plant Journal **44**, 1054–1064.

Fong Y, Chongzhi D, Huang Y, Gilbert PB. 2017*a*. Model-robust Inference for Continuous Threshold Regression Models. Biometrics, 452–462.

Fong Y, Huang Y, Gilbert PB, Permar SR. 2017*b*. chngpt: Threshold regression model estimation and inference. BMC Bioinformatics **18**, 1–7.

Forsythe WC, Rykiel EJ, Stahl RS, Wu H i., Schoolfield RM. 1995. A model comparison for daylength as a function of latitude and day of year. Ecological Modelling **80**, 87–95.

Guo T, Wei J, Li X, Yu J. 2023. Environmental context of phenotypic plasticity in flowering time in sorghum and rice. Journal of Experimental Botany doi: 10.1093/jxb/erad398.

Harrison MT, Tardieu F, Dong Z, Messina CD, Hammer GL. 2014. Characterizing drought stress and trait influence on maize yield under current and future conditions. Global Change Biology **20**, 867–878.

Herrero MP, Johnson RR. 1981. Drought Stress and Its Effects on Maize Reproductive Systems 1 . Crop Science **21**, 105–110.

Hung HY, Shannon LM, Tian F, *et al.* 2012. ZmCCT and the genetic basis of day-length adaptation underlying the postdomestication spread of maize. Proceedings of the National Academy of Sciences of the United States of America **109**.

Itoh H, Nonoue Y, Yano M, Izawa T. 2010. A pair of floral regulators sets critical day length for Hd3a florigen expression in rice. Nature Genetics **42**, 635–638.

Izawa T. 2021. What is going on with the hormonal control of flowering in plants? Plant Journal **105**, 431–445.

Jarquín D, Crossa J, Lacaze X, *et al.* 2014. A reaction norm model for genomic selection using high-dimensional genomic and environmental data. **127**, 595–607.

Jin M, Liu H, Liu X, *et al.* 2023. Complex genetic architecture underlying the plasticity of maize agronomic traits. Plant Communications **4**, 100473.

Johansson M, Staiger D. 2015. Time to flower: Interplay between photoperiod and the circadian clock. Journal of Experimental Botany **66**, 719–730.

Kiniry JR. 1991. Maize phasic development. American Society of Agronomy, 55–70.

Kiniry JR, Ritchie JT, Musser RL. 1983*a*. Dynamic Nature of the Photoperiod Response in Maize. **10**, 10–13.

Kiniry JR, Ritchie JT, Musser RL, Flint EP, Iwig WC. 1983*b*. The Photoperiod Sensitive Interval in Maize. Agronomy Journal **75**, 687–690.

Kusmec A, Srinivasan S, Nettleton D, Schnable PS. 2017. Distinct genetic architectures for phenotype means and plasticities in Zea mays. Nature Plants **3**, 715–723.

Lee SH, Choi CW, Park KM, *et al.* 2021. Diversification in Functions and Expressions of Soybean FLOWERING LOCUS T Genes Fine-Tunes Seasonal Flowering. Frontiers in Plant Science **12**, 1–16.

Lee JH, Ryu H-S, Chung KS, Posé D, Kim S, Schmid M, Ahn JH. 2013. Regulation of Temperature-Responsive Flowering by MADS-Box Transcription Factor Repressors. Science **342**, 628–632.

Lejeune P, Bernier G. 1996. Effect of environment on the early steps of ear initiation in maize (Zea mays L.). Plant, Cell and Environment **19**, 217–224.

McFarland BA, Alkhalifah N, Bohn M, *et al.* 2020. Maize genomes to fields (G2F): 2014-2017 field seasons: Genotype, phenotype, climatic, soil, and inbred ear image datasets. BMC Research Notes **13**, 4–9.

Millet EJ, Kruijer W, Coupel-Ledru A, Alvarez Prado S, Cabrera-Bosquet L, Lacube S, Charcosset A, Welcker C, van Eeuwijk F, Tardieu F. 2019. Genomic prediction of maize yield

660 across European environmental conditions. Nature Genetics **51**, 952–956.

661 **Minow MAA, Ávila LM, Turner K, Ponzoni E, Mascheretti I, Dussault FM, Lukens L, Rossi V,**
662 **Colasanti J**. 2018. Distinct gene networks modulate floral induction of autonomous maize and
663 photoperiod-dependent teosinte. Journal of Experimental Botany **69**, 2937–2952.

664 **Muller B, Martre P**. 2019. Plant and crop simulation models: Powerful tools to link physiology,
665 genetics, and phenomics. Journal of Experimental Botany **70**, 2339–2344.

666 **Padilla JM, Otegui ME**. 2005. Co-ordination between leaf initiation and leaf appearance in field-
667 grown maize (Zea mays): Genotypic differences in response of rates to temperature. Annals of
668 Botany **96**, 997–1007.

669 **Parent B, Tardieu F**. 2012. Temperature responses of developmental processes have not been
670 affected by breeding in different ecological areas for 17 crop species. New Phytologist **194**, 760–774.

671 **Parent B, Turc O, Gibon Y, Stitt M, Tardieu F**. 2010. Modelling temperature-compensated
672 physiological rates, based on the co-ordination of responses to temperature of developmental
673 processes. Journal of Experimental Botany **61**, 2057–2069.

674 **Rising J, Devineni N**. 2020. Crop switching reduces agricultural losses from climate change in the
675 United States by half under RCP 8.5. Nature Communications **11**, 1–7.

676 **Rogers AR, Dunne JC, Romay C, *et al.*** 2021. The importance of dominance and genotype-by-
677 environment interactions on grain yield variation in a large-scale public cooperative maize
678 experiment. G3: Genes, Genomes, Genetics **11**.

679 **Rood SB, Major DJ**. 1980. Responses of Early Corn Inbreds to Photoperiod. Crop Science **20**, 679–
680 682.

681 **Roof DA**. 1997. *Evolutionary quantitative genetics*.

682 **Simpson GG, Dean C**. 2002. Arabidopsis, the Rosetta Stone of Flowering Time ? Science **296**, 285–
683 289.

684 **Sloat LL, Davis SJ, Gerber JS, Moore FC, Ray DK, West PC, Mueller ND**. 2020. Climate
685 adaptation by crop migration. Nature Communications **11**, 1–9.

686 **Sparks A**. 2018. nasapower: A NASA POWER Global Meteorology, Surface Solar Energy and
687 Climatology Data Client for R. Journal of Open Source Software **3**, 1035.

688 **Srikanth A, Schmid M**. 2011. Regulation of flowering time: All roads lead to Rome. Cellular and
689 Molecular Life Sciences **68**, 2013–2037.

690 **Teixeira JEC, Weldekidan T, De Leon N, *et al.*** 2015. Hallauer's Tusón: A decade of selection for
691 tropical-to-temperate phenological adaptation in maize. Heredity **114**, 229–240.

692 **Tenaillon MI, Charcosset A**. 2011. A European perspective on maize history. Comptes Rendus -
693 Biologies **334**, 221–228.

694 **van Voorn GAK, Boer MP, Truong SH, Friedenberg NA, Gugushvili S, McCormick R, Bustos**
695 **Korts D, Messina CD, van Eeuwijk FA**. 2023. A conceptual framework for the dynamic modeling
696 of time-resolved phenotypes for sets of genotype-environment-management combinations: a model
697 library. Frontiers in Plant Science **14**, 1–14.

698 **Wang E, Engel T**. 1998. Simulation of phenological development of wheat crops. Agricultural
699 Systems **58**, 1–24.

700 **Wang E, Martre P, Zhao Z, *et al.*** 2017. The uncertainty of crop yield projections is reduced by
701 improved temperature response functions. Nature Plants **3**, 1–11.

Yang Q, Li Z, Li W, *et al.* 2013. CACTA-like transposable element in ZmCCT attenuated photoperiod sensitivity and accelerated the postdomestication spread of maize. Proceedings of the National Academy of Sciences of the United States of America **110**, 16969–16974.

Yang N, Wang Y, Liu X, *et al.* 2023. Two teosintes made modern maize. Science **382**, 1013–1021.

Yanovsky MJ, Kay SA. 2003. Living by the calendar: How plants know when to flower. Nature Reviews Molecular Cell Biology **4**, 265–275.

Zabel F, Müller C, Elliott J, *et al.* 2021. Large potential for crop production adaptation depends on available future varieties. Global Change Biology **27**, 3870–3882.

List of Tables and Figures

Table 1. Distribution percentiles for the basic vegetative phase and leaf tip appearance at tassel initiation of panel 1.

Table 2. Impact of latent variable adjustment on PRN-FTP parameter estimation for different maize lines.

Figure 1. Envirotyping of sensed photoperiod across and within maize fields in the Northern Hemisphere.

Figure 2. Adjusting for latent variable effects across a multi-environment trial network when fitting the PRN-FTP.

Figure 3. The PRN-FTP for seven tropical lines of maize.

Figure 4. The trait space for flowering time *per se* and photoperiod sensitivity in a diversity panel of maize.

723 **Table 1. Percentiles of the distribution for the basic vegetative phase at tassel initiation (BVP-ti)**
724 **in panel 1.**

	Min	**5%**	**25%**	**50%**	**75%**	**95%**	**Max**
BVP-ti (ºCd)	169	239	286	326	375	434	496

725

726 **Table 2. Impact of latent variable adjustment and genotype-specific envirotyping on PRN-FTP**
727 **parameter estimation for different maize lines.**

Genotype	Intercept (ºCd)	Threshold (h)	Slope (ºCd h^{-1})	RMSE
Unadjusted values with genotype-specific *DL*^{s}				
CML10	851.0 ± 28.6	12.3 ± 0.6	44.3 ± 9.7	82.0
CML258	934.6 ± 33.4	12.3 ± 0.7	42.1 ± 11.4	95.4
CML277	856.5 ± 22.1	14.5 ± 0.6	96.7 ± 18.7	76.0
CML341	802.0 ± 24.7	12.3 ± 0.6	49.1 ± 8.4	71.2
CML373	815.2 ± 30.6	12.3 ± 1.1	35.9 ± 10.7	67.5
Tzi8	858.0 ± 29.1	12.4 ± 1.1	30.9 ± 9.9	86.4
Tzi9	809.0 ± 29.5	12.2 ± 1.1	26.3 ± 9.3	85.0
Adjusted values with genotype-specific *DL*^{s}				
CML10	872.8 ± 16.7	12.3 ± 0.6	36.9 ± 5.6	47.7
CML258	953.8 ± 21.2	12.3 ± 0.9	37.7 ± 7.2	60.5
CML277	869.8 ± 9.2	14.5 ± 0.6	87.7 ± 8.0	31.3
CML341	846.0 ± 9.8	14.3 ± 0.6	86.7 ± 7.9	33.8
CML373	853.1 ± 11.6	12.3 ± 0.8	26.4 ± 4.0	25.6
Tzi8	888.8 ± 14.7	14.3 ± 1.0	44.3 ± 10.7	52.8
Tzi9	842.1 ± 11.2	14.4 ± 0.9	41.8 ± 8.8	40.0
Adjusted values with common reference *DL*^{s}				
CML10	873.7 ± 16.5	12.3 ± 0.6	37.5 ± 5.7	47.6
CML258	955.8 ± 21.0	12.3 ± 0.9	37.7 ± 7.3	60.5
CML277	870.2 ± 9.3	14.3 ± 0.5	77.0 ± 7.1	32.1
CML341	846.9 ± 9.9	14.3 ± 0.6	83.2 ± 7.6	34.2
CML373	853.5 ± 11.5	12.2 ± 0.8	26.3 ± 4.0	25.5
Tzi8	888.6 ± 14.7	14.5 ± 1.1	47.9 ± 11.6	52.8
Tzi9	841.9 ± 11.2	14.5 ± 0.8	43.2 ± 9.0	39.9

728 Root mean squared error (RMSE) is reported for the full bilinear model.

Figure 1. Envirotyping of sensed photoperiod across and within maize fields in the Northern Hemisphere.

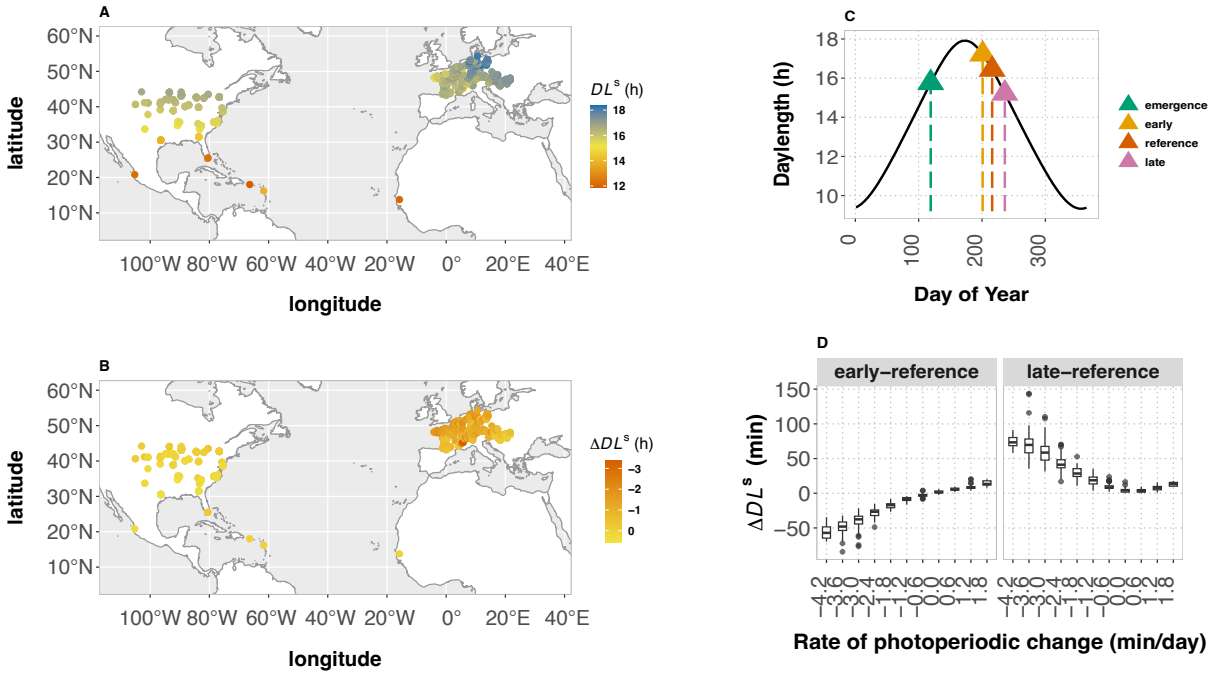

(A) Sensed photoperiod (DL^s for the 50th percentile maturity reference) across maize field sites in the Northern Hemisphere. (B) Within environment differences in hours of sensed daylength (ΔDL^s) between the 95th and 5th percentile maturity groups defined by the BVP-ti distribution of panel 1. (C) The figure portrays how different maturity groups can reach the photoperiod sensitized stage on different days of the year within the same environment, leading to differences in DL^s (the 5th, 50th, and 95th percentile values of the BVP-ti in panel 1are indicated as early, reference, and late maturity groups) (D) The relationship between within environment differences in DL^s and rates of daily photoperiodic change. Here, the differences are shown in minutes for comparisons between the reference maturity group relative to the early and late maturity groups. As reflected in (B), the boxplots show that genotypes within the same environment experience increasingly greater differences in photoperiods when rates of photoperiodic change increase, which occurs in association with increasing latitude.

Figure 2. Adjusting for latent variable effects across a multi-environment trial network when fitting the PRN-FTP.

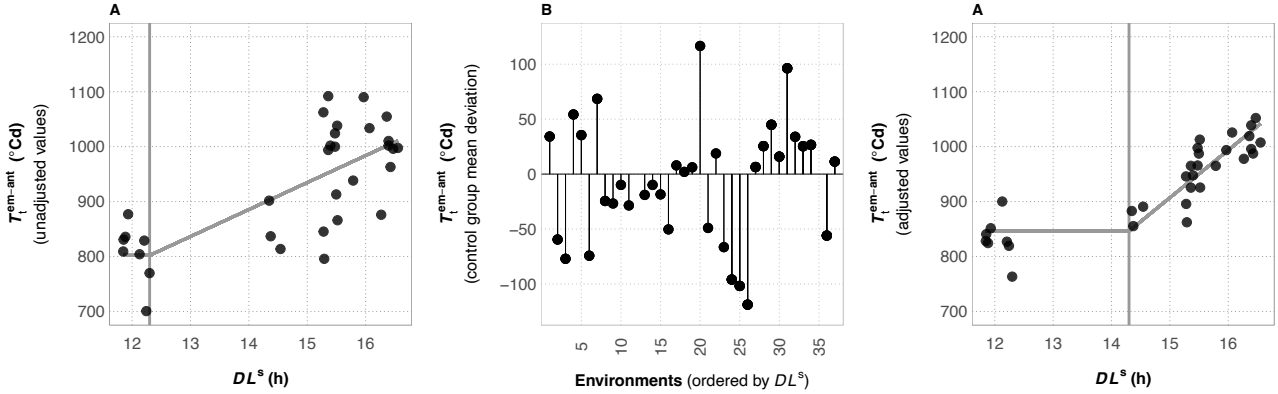

(A) The plot shows the PRN-FTP for genotype CML341, using unadjusted BLUEs for thermal time from crop emergence to anthesis (T_t^{em-ant}; black points). The grey lines show the estimated flowering time *per se* (horizontal line), critical threshold value (vertical line), and photoperiod sensitivity (sloped line). (B) Deviations from the overall average T_t^{em-ant} for the control groups of photoperiod insensitive lines estimated across the same environments, with the environment identifiers ordered as in panels (A) and (B) according to sensed daylength (DL^s). (C) The PRN-FTP for genotype CML341 after adjusting the BLUEs by deviations in (B), leading to different estimates for the flowering time *per se*, the critical threshold value, and the photoperiod sensitivity.

Figure 3. The PRN-FTP for seven tropical lines of maize.

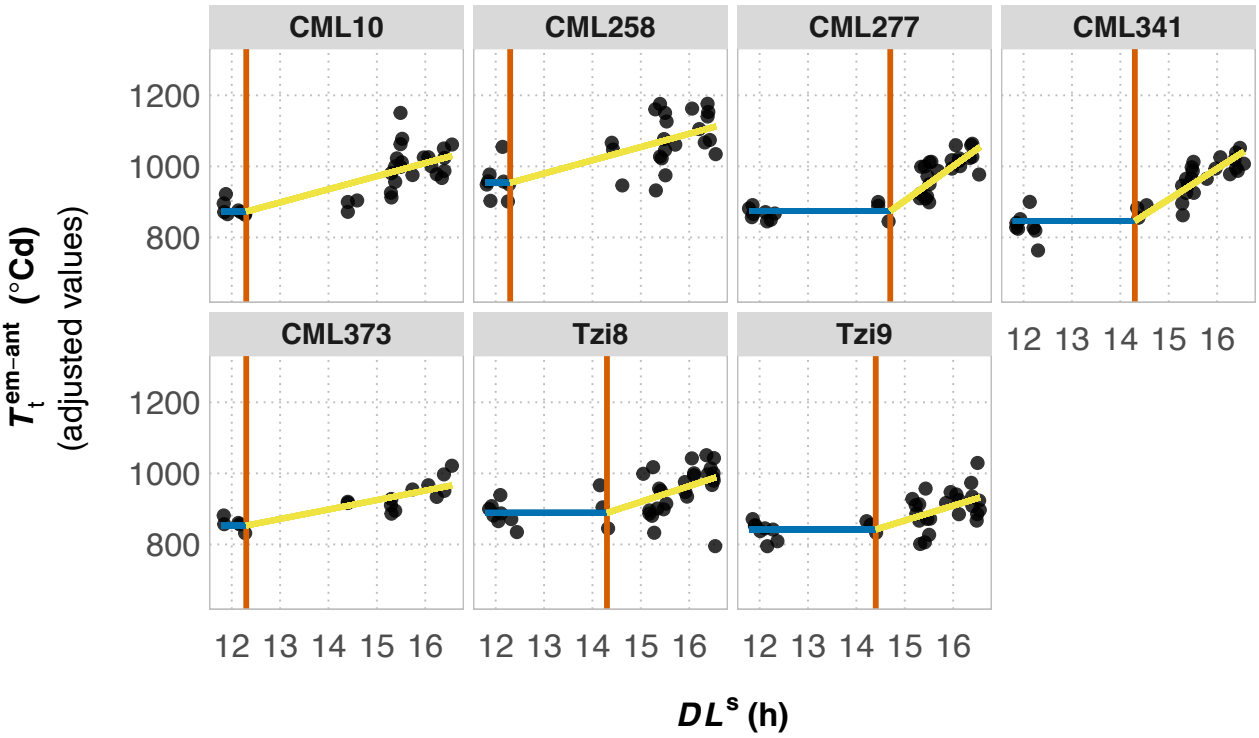

(A) For each genotype, the plots show the three PRN-FTP parameters estimated from the bilinear function fitted using latent-variable adjusted BLUEs for thermal time from crop emergence to anthesis (T_t^{em-ant}) in relation to sensed daylength (DL^s). Parameter estimates are shown for the flowering time *per se* (blue line), the critical threshold value (red line), and the photoperiod sensitivity (yellow line).

761 **Figure 4. The trait space for flowering time *per se* and photoperiod sensitivity in a diversity panel**
762 **of maize.**

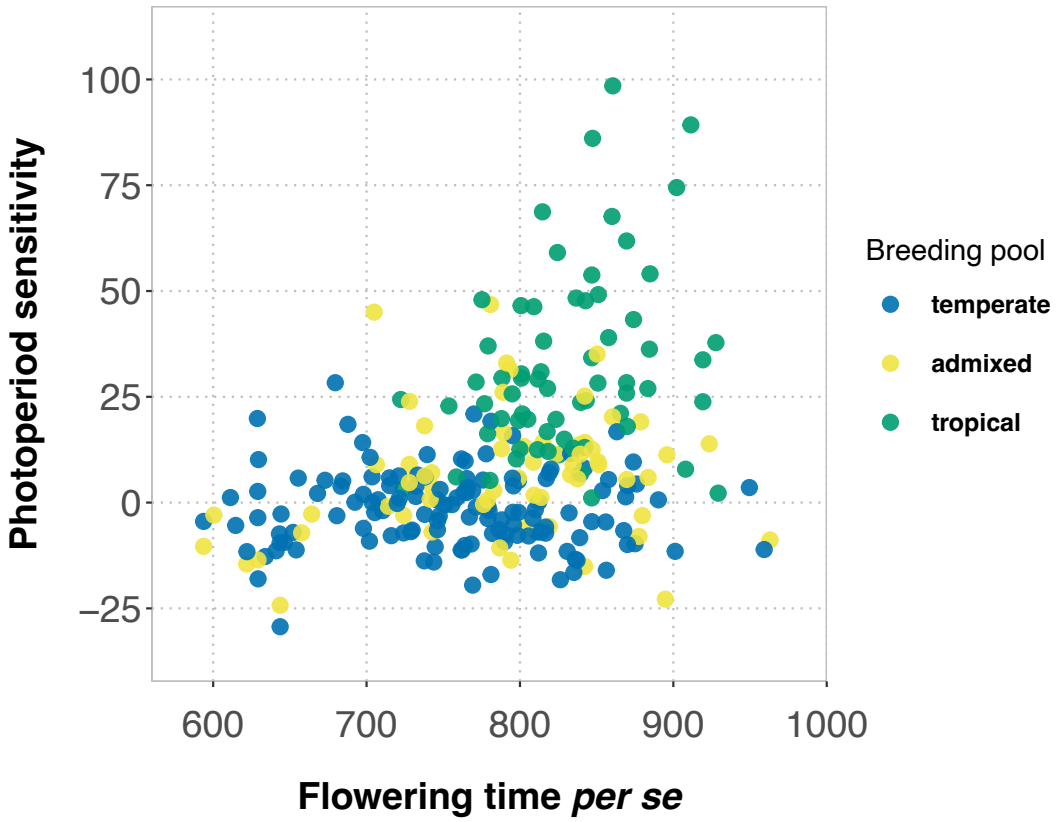

763

764 Points correspond to genotypic values for flowering time *per se* (ºCd) and photoperiod sensitivity
765 (ºCd h^{-1}), estimated using the LD-SD regression method on latent-variable adjusted BLUEs.
766 Breeding pools are represented by samples of inbred lines previously assigned to temperate (n=137),
767 admixed (n=62), and tropical (n=66) sources based on structure analysis of marker data (Flint-Garcia
768 *et al.*, 2005).